Stress Metrology : The challenge for the next generation of engineered wafers

Antoine Tiberj, Vincent Paillard, Cécile Aulnette, Nicolas Daval, Myriam Moreau, Mark Kennard, Ian Cayrefourcq, Konstantin K. Bourdelle

Stress Metrology : The challenge for the next generation of engineered wafers

Antoine Tiberj[a], Vincent Paillard[b], Cécile Aulnette[a], Nicolas Daval[a], Konstantin K. Bourdelle[a], Myriam Moreau[c], Mark Kennard[a] and Ian Cayrefourcq[a]
[a]Soitec, Parc technologique des Fontaines, 38190 Bernin France.
[b]LPST, Paul Sabatier University, 118 route de Narbonne, 31062 Toulouse Cedex 4, France.
[c]Jobin-Yvon, 231 rue de Lille, 59650 Villeneuve d'Ascq, France.

ABSTRACT

Raman spectroscopy is a powerful and versatile technique for stress measurements in complex stacks of thin crystalline layers at macroscopic and microscopic scales. Using such a technique we show that thick SiGe layers epitaxially grown using graded buffer method are fully relaxed (>95%) at a macroscopic scale but exhibit a small strain modulation at a microscopic scale. For the first time we report the results of Raman micro-mapping of stress distribution in SGOI wafers produced by Smart Cut™ technology. We conclude that Smart Cut™ is a unique method to manufacture the next generation of engineered wafers that can combine strained and/or relaxed SiGe alloys, Si and Ge films, while keeping their initial strain properties at both scales. It is important to develop Raman spectroscopy tool for in-line process control in fabrication of strained Silicon On Insulator (sSOI) wafers.

INTRODUCTION

As scale reduction of devices becomes increasingly challenging from a technological point of view, the use of new materials that can improve circuit performance is of great interest. Strained silicon films on insulator are often identified as the engineered wafers needed for the 65 nm CMOS technology node and beyond. They combine the advantages coming from the buried insulator and the strained silicon layers [1]. The wafers can be produced either with (SGOI) or without (sSOI) a relaxed SiGe layer between the strained silicon and the buried insulator films. The unique feature of the Smart Cut™ technology enables transfer of a thin film (of essentially any crystalline material) coming from a donor wafer onto an insulating layer to produce the final semiconductor on insulator wafer [2]. Therefore the Smart Cut™ technology is a powerful method to manufacture the next generation of engineered wafers combining all sorts of strained and/or relaxed SiGe alloys, sSi and Ge films on insulators.
For the development of the sSOI process flow the stress metrology is of critical importance. The experimental technique chosen must determine with high precision the Ge composition and the degree of relaxation of SiGe films as well as the stress induced in the top silicon film. It should be fast, clean-room compatible and be easily adapted in the in-line metrology tool. Standard profiling techniques can not fulfil all these requirements. Spectroscopic Ellipsometry (SE) can measure the SiGe composition due to the refractive index changes [3]. However, SE ability to measure the strain in Si films is still to be demonstrated (the analysis of birefringence effects might address this challenge [4,5]).
X-ray diffraction (XRD) and Raman spectroscopy seem to be better positioned to address the stress metrology issue. XRD is the only technique that images directly the crystalline lattice. The composition and the residual strain of an epitaxial SiGe layer is determined using well known methods developed by J. Hornstra and W.J. Bartels in 1978 [6,7] and applied to SiGe alloys by M. Fatemi and R.E Stahlbush [8].XRD, however, is time-consuming, has a limited spatial resolution and the analysis becomes difficult for the thin and/or bonded layers. Investigation of

thin layers (< 20 nm) requires either synchrotron facilities [9] or grazing incidence analysis. Both approaches are detrimental for the spatial resolution of the technique. In addition, the bonded layers generally have some misorientation between the top film and the substrate coming from the miscut of the wafers. That makes the stress determination in the top film time consuming and cumbersome [10,11].

RAMAN SPECTROSCOPY

Raman spectroscopy has demonstrated its high sensitivity to measure stress in cubic semiconductors and especially in silicon layers [12] by probing the optical phonons shifts [13,14,15,16] that are directly related to the stress applied to the crystal. Raman spectroscopy benefits from a high spatial resolution, high throughput and high versatility. The laser wavelength can be easily changed to probe only the desired thickness. Use of UV lasers enables one to measure very thin silicon layers and to benefit from resonance effects [17,18].
The technique provides the measurements of the Ge composition and the residual strain in SiGe alloys. E.g., J. C. Tsang et al. [19] described the method based on the measurements of three different Raman modes related to the Si-Si, Si-Ge and Ge-Ge bonds. The frequency of these three modes directly depends on the Ge content and the strain of the SiGe layers through the following relationships :

$$\omega_{SiSi} = 521 - 68\,x - 815\,\varepsilon_{//} \quad (1)$$

$$\omega_{SiGe} = 399.5 + 14.2\,x - 575\,\varepsilon_{//} \quad (2)$$

$$\omega_{GeGe} = 282.5 + 16\,x - 385\,\varepsilon_{//} \quad (3)$$

The numerical coefficients were determined experimentally and calibrated with HRXRD and SIMS measurements. A controversy still exists regarding the exact values [19,20]. However, we will use the relationships (1) and (2) which enable us to measure accurately the Ge content x and to derive the degree of relaxation:

$$\text{degree of relaxation} = 1 - \frac{\varepsilon_{// \exp}}{\varepsilon_{// th}} \quad (4)$$

where $\varepsilon_{// \exp}$ is the residual strain measured and $\varepsilon_{// th}$ is the theoretical strain of a fully relaxed SiGe layer having a composition x of Ge.
The high spatial resolution of Raman spectroscopy is demonstrated by the observation of the strain network induced by the misfit dislocations buried in the relaxed SiGe buffer [21]. This strain network influences the growth rate of SiGe layers [22] and might explain the formation of the well-known crosshatch surface morphology [23,24]. In fact, the crosshatch in SiGe layers develops through the combination of two mechanisms depending on the film thickness: dislocation-induced surface steps due to shear displacements caused by dislocations glide and the growth of self-organized periodic ridges [25,26,27]. The presence of the strain network and the buried misfits was also observed by: (1) the broadening of the SiGe XRD peaks [27], (2) the high-resolution-channelling contrast microscopy where an increase in the channelling yield χ_{min} due to a slight lattice tilt was detected [28], and (3) by polarized Near-field Scanning Optical Microscope (NSOM) where photocurrent variations due to local changes in band structure were observed [29]. For the device applications it is important to study this strain network and its influence on the device electrical parameters. We demonstrated recently that Smart Cut^{TM} technology keeps the macroscopic stress of the starting sSi layer in the final sSOI wafer [30,31]. It is also important to know if the microscopic strain modulation is affected by the process steps involved in the sSOI and SGOI Smart Cut^{TM} wafer manufacturing.

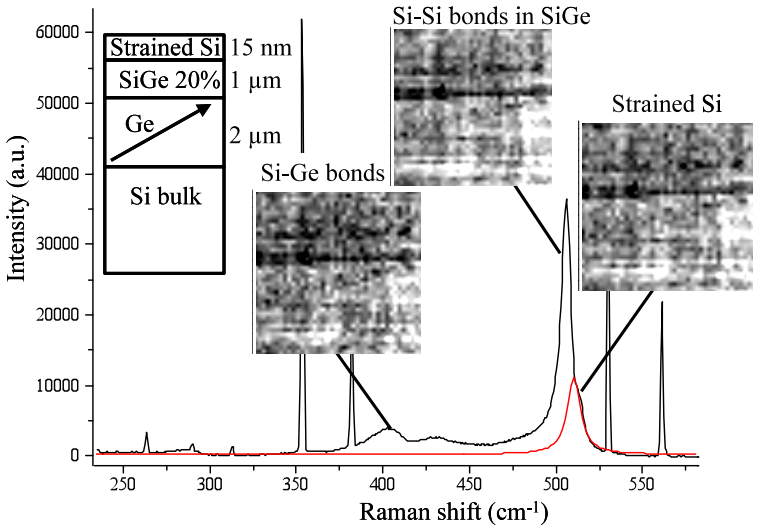

Figure 1. Raman spectrum of a strained silicon film grown on top of relaxed SiGe buffer. We clearly observe two typical SiGe Raman modes coming from Si-Ge (400 cm^{-1}) and Si-Si (508 cm^{-1}) bonds. The signal due to the strained Si film is seen as a shoulder on the right hand side of the Si-Si bond signal. The sharp lines in the spectrum correspond to the elastically scattered plasma lines of the Argon laser . We used them as a frequency reference. We performed a Raman mapping (40 x 40 μm^2) of the sample and plotted the spatial variation of the SiGe and strained Si Raman modes.

EXPERIMENTAL RESULTS

We studied two types of wafers: a donor wafer with a strained Si cap grown on a relaxed $Si_{0.8}Ge_{0.2}$ buffer and a SGOI wafer. We used a Labram HR spectrograph and the set-up with the 488 nm wavelength of an Ar laser at Jobin-Yvon demo laboratory. First, Raman mapping was performed on the donor wafer, to confirm previously published results [21,22] and to calibrate the relationships used in our analysis. Figure 1 depicts the layer stack studied, the typical Raman spectrum collected and the Raman maps. Raman shifts variations of both films (SiGe and strained Si) are plotted and exhibit the same crosshatch pattern. All the Raman modes (and especially the Si-Ge and Si-Si bonds of the SiGe film) shift coherently depending on the laser beam position on the sample. Analysis based on relationships (1-3) shows that this variation can only come from strain variation in the SiGe layer (and not variation in the Ge content). As the laser penetration depth is around 500 nm, we do not observe the strain field in the vicinity of the misfit dislocations like authors [21] but rather the strain distribution close to the surface [22]. From the Raman shifts we can directly determine the stress in the strained Si layer, the composition and the degree of relaxation of the SiGe layer. From the SiGe composition and residual strain we can then calculate the SiGe lattice parameter and the stress it must induce in the top Si layer. We show these four maps in Figure 2. In order to eliminate the experimental artefacts we also obtained Raman maps after a 45° rotation of the sample. The strain field observed in the Si cap is aligned with the <110> crystalline directions like the crosshatch and the misfit dislocations network and comes directly from the variation in the SiGe layer. These results confirm that the Ge content is uniform but the SiGe layer is not fully relaxed although HRXRD results showed relaxation higher than 95%. We compared directly the stress the SiGe layer must induce in the strained Si cap to the measured value and got a perfect agreement. The difference

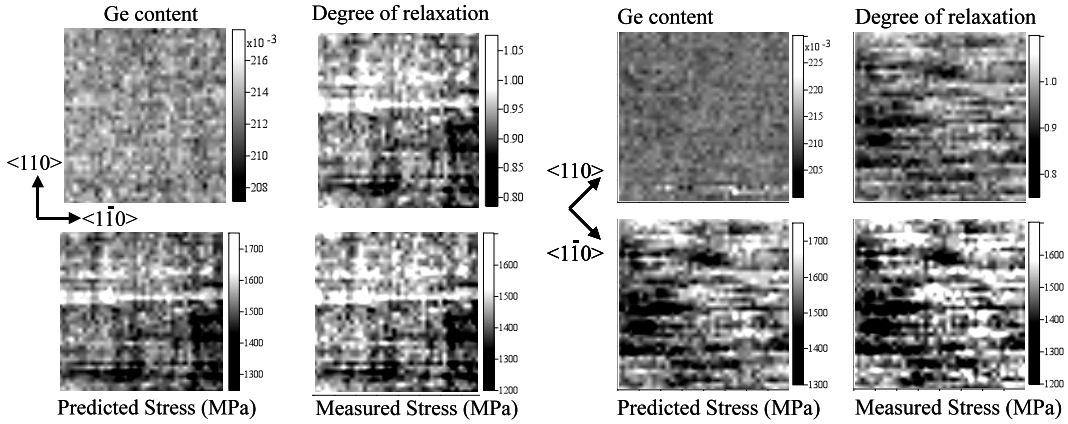

Figure 2. Two Raman maps were obtained for the donor wafer with two different orientations (0° on left hand side and 45° on the right hand side). The area of the 0° and 45° map is respectively 40 x 40 μm^2 and 20 x 20 μm^2. We show the spatial variations of the Ge content and the degree of relaxation of the SiGe layer in the top maps. From the SiGe layer properties we calculated the SiGe lattice parameter and the stress it must induce to the strained Si cap. In the bottom maps, we compare the predicted stress and the measured stress. We observe a perfect agreement. The stress difference is lower than 100 MPa for all points in the map.

between the predicted and measured stress is lower than 100 MPa. It confirms the validity of the relationships used and the perfect lattice matching between the Si cap and the SiGe strain-relaxed buffer. No misfit dislocations were observed at the sSi/SiGe interface by TEM analysis.
We measured then an SGOI wafer fabricated with the Smart Cut^{TM} technology. The layer stack and a typical Raman spectrum for this wafer is shown in Figure 3. Since the SiGe layer in this case is significantly thinner (around 35 nm) the SiGe Raman modes are weaker because of the laser penetration depth. The laser wavelength needs to be adjusted to the studied layer thickness in order to optimize the signal to noise ratio. An additional Raman mode is observed : the Si Raman mode coming from the Si bulk wafer. The Raman mapping exhibits the same strain network pattern in the transferred SiGe layer and in the strained Si cap grown on the SiGe layer (see Figure 4). After performing the previously described analysis of the Raman shifts we deduced the composition and the degree of relaxation of the SiGe layer which is in perfect

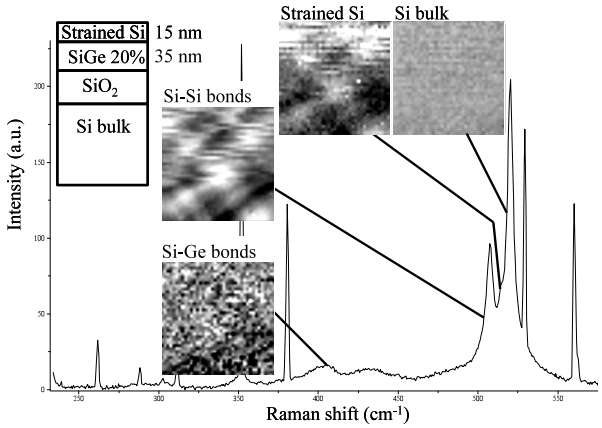

Figure 3. SGOI Raman spectrum exhibiting the Raman modes from the sSi cap, the thin SiGe layer and the underlying Si handle wafer. The strained Si and SiGe layers demonstrate the crosshatched strain network. The stress in the Si handle wafer is weak (100 MPa) and uniform.

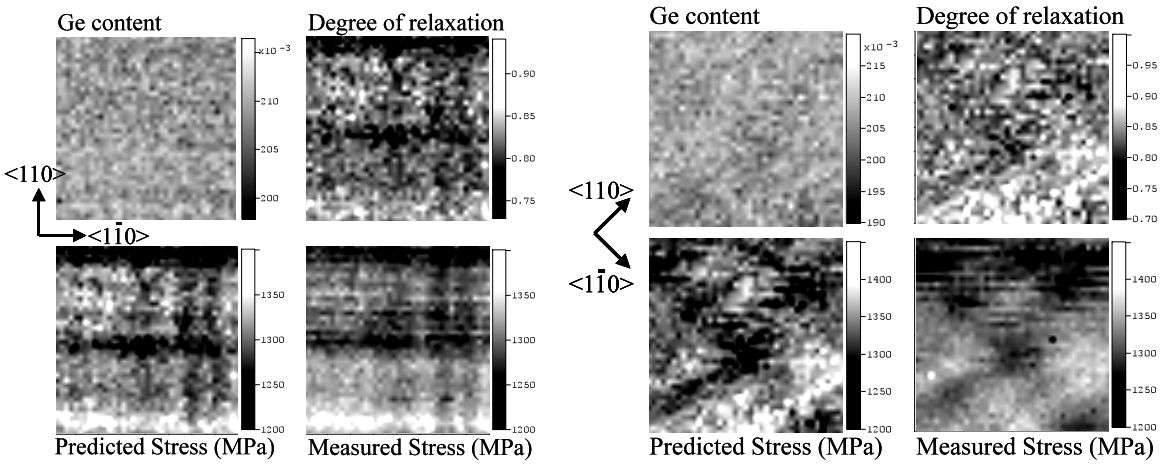

Figure 4. Two Raman mapping were performed on the SGOI wafer with two different orientations (0° on left hand side and 45° on the right hand side). The size of the 0° and 45° map are respectively 40 x 40 µm and 20 x 20 µm. We plotted the spatial variations of the Ge content, the degree of relaxation of the SiGe layer on the upper maps. On the lower maps, we compare the predicted stress to the stress measured in the Si cap. We got a perfect agreement. The stress difference is lower than 100 MPa at all point of the map.

agreement with the stress measured in the sSi cap. The difference between the predicted and measured stress is still lower than 100 MPa and shows the perfect lattice matching between the SiGe and the sSi films without misfit dislocations nucleation. We also observed a very small, around 100 MPa, tensile stress in the Si handle wafer due to the difference between thermal expansion coefficients of the buried oxide and silicon [11,32]. The stress in the Si handle wafer is weak, uniform and does not vary across the wafer. We state that Smart Cut™ can be applied to the transfer of any combination of strained and/or relaxed layers without changing the stress properties even at the microscopic scale.

CONCLUSIONS

We demonstrated that constant composition SiGe layers epitaxially grown on relaxed SiGe graded buffers are fully relaxed, >95%, at a macroscopic scale. On a microscopic scale, however, these SiGe layers exhibit a small strain modulation aligned with the <110> crystalline directions with a spatial wavelength in the range of 10 µm. The modulations influence the SiGe growth and the crosshatch surface morphology formation. They also impact the strained Si cap grown on such buffers. The stress fluctuation in the sSi film reported in this work and the previously published papers [21,22] is about 250 MPa.

We showed that Smart Cut™ technology preserves the stress properties of the transferred layers on macroscopic [31] and microscopic scales. The results discussed here pose important questions whether the different SiGe epitaxy recipes and/or FEOL processes (during device fabrication) will affect the microscopic strain distribution. For the device manufacturers, one of the concerns related to the present observations is whether the strain network will cause significant fluctuation in the electrical parameters of the devices. The impact of the stress variation on device parameters is difficult to evaluate since, e.g., even the mechanisms of the electron and hole mobility improvements in sSi are not well understood [33]. We believe that it is possible to define the process window where the small strain fluctuations will not impact the mobility, i.e. by choosing the strain level where the mobility improvements saturate.

REFERENCES

1 G.K. Celler and S. Cristoloveanu, J. Appl. Phys. **93**, 4955 (2003).
2 B. Ghyselen, *Wafer Bonding VII : Science, Technology and Applications*, p. 96 , ECS Proceedings (PV 2003-19, ISBN 1-56677-402-0), Pennington, NJ (2003).
3 C. Pickering and R.T. Carline, J. Appl. Phys. **75**, 4642 (1994).
4 S. Mukerjee and V. Venkataraman, Appl. Phys. Lett. **77**, 3529 (2000).
5 D.K. Biegelsen, Phys. Rev. Lett. **32**, 1196 (1974).
6 J. Hornstra and W.J. Bartels, J. Cryst. Growth **44**, 513 (1978).
7 W.J. Bartels and W. Nijman, J. Cryst. Growth **44**, 518 (1978).
8 M. Fatemi and R.E. Stahlbush, Appl. Phys. Lett. **58**, 825 (1991).
9 P.M. Mooney et al., AIP Conference Proceedings **683**, 213 (2003).
10 G.M. Cohen et al., Appl. Phys. Lett. **75**, 787 (1999).
11 A. Tiberj, B. Fraisse, C. Blanc, S. Contreras, J. Camassel, Phys. Stat. Sol. (c) **0**, 1060 (2003).
12 I. De Wolf, Semicond. Sci. Technol. **11**, 139 (1996).
13 E. Anastassakis, A. Pinczuk, E. Burstein, F.H. Pollak and M. Cardona, Solid State Comm. **8**, 133 (1970).
14 F. Cerdeira, C.J. Buchenauer, F.H. Pollak and M. Cardona, Phys. Rev. B **5**, 580 (1972).
15 E. Anastassakis, A. Cantarero and M. Cardona, Phys. Rev. B **41**, 7529 (1990).
16 E. Anastassakis, J. Appl. Phys. **82**, 1582 (1997).
17 V. Paillard, M.A. Laguna, P. Puech, P. Temple-Boyer, B. Caussat, J.P. Couderc, B. De Mauduit, Appl. Phys. Lett. **73**, 1718-1720 (1998).
18 J.B. Renucci, R.N. Tyte and M. Cardona, Phys. Rev. B **11**, 3885 (1975).
19 J.C. Tsang, P.M. Mooney, F. Dacol and J.O Chu, J. Appl. Phys. **75**, 8098 (1994).
20 J. Groenen et al., Appl. Phys. Lett. **71**, 3856 (1997).
21 H. Chen et al., Phys. Rev. B **65**, 233303 (2002).
22 K. Sawano, S. Koh, Y. Shiraki, N. Usami, K. Nakagawa, App. Phys. Lett. **83**, 4339 (2003).
23 J.W.P. Hsu, E.A. Fitzgerald, Y.H. Xie, P.J. Silverman and M.J. Cardillo, Appl. Phys. Lett. **61**, 1293 (1992).
24 J.M. Hartmann, B. Gallas, J. Zhang and J.J. Harris, Semicond. Sci. Technol. **15**, 370 (2000).
25 S.Y. Shiryaev, F. Jensen and J.W. Petersen, Appl. Phys. Lett. **64**, 3305 (1994).
26 M. Kummer, B. Vögeli, T. Meyer and H. Van Känel, Phys. Rev. Lett. **84**, 107 (2000).
27 T. Spila, P. Desjardins, J. D'Arcy-Gall, R.D. Twesten and J.E. Greene, J. Appl. Phys. **93**, 1918 (2003).
28 H.L. Seng, T. Osipowicz, T.C. Sum, E.S. Tok, G. Breton, N.J. Woods and J. Zhang, Appl. Phys. Lett. **80**, 2940 (2002).
29 M.H. Gray, J.W.P. Hsu, L. Giovane and M.T. Bulsara, Phys. Rev. Lett. **86**, 3598 (2001).
30 B. Ghyselen et al., Proceedings of the ICSi3 Conference, Santa Fe (NM, USA), Mars 2003.
31 B. Ghyselen et al., Solid State Electronics, in press (August 2004).
32 A. Tiberj, J. Camassel, N. Planes, Y. Stoemenos, H. Moriceau and O. Rayssac, *SOI Technology and Devices XI*, p. 117 , ECS Proceedings (PV 2003-05, ISBN 1-56677-375-X), Pennington, NJ (2003).
33 M.V. Fischetti, F. Gamiz and W. Hänsch, J. Appl. Phys. **92**, 7320 (2002).